Large-Scale Fusion of Gray Matter and Resting-State Functional MRI Reveals Common and Distinct Biological Markers across the Psychosis Spectrum in the B-SNIP Cohort

frontiers in Psychiatry

ORIGINAL RESEARCH
published: 21 December 2015
doi: 10.3389/fpsyt.2015.00174

Large-Scale Fusion of Gray Matter and Resting-State Functional MRI Reveals Common and Distinct Biological Markers across the Psychosis Spectrum in the B-SNIP Cohort

Zheng Wang[1], Shashwath A. Meda[2], Matcheri S. Keshavan[3], Carol A. Tamminga[4], John A. Sweeney[4], Brett A. Clementz[5], David J. Schretlen[6], Vince D. Calhoun[6,7,8], Su Lui[9] and Godfrey D. Pearlson[2,8]*

[1] Mental Health Institute of the Second Xiangya Hospital, Central South University, Changsha, China, [2] Olin Neuropsychiatry Research Center, Institute of Living at Hartford Hospital, Hartford, CT, USA, [3] Department of Psychiatry, Beth Israel Deaconess Hospital, Harvard Medical School, Boston, MA, USA, [4] Department of Psychiatry, University of Texas Southwestern Medical Center, Dallas, TX, USA, [5] Department of Psychology, University of Georgia, Athens, GA, USA, [6] Department of Psychiatry, Johns Hopkins University, Baltimore, MD, USA, [7] The Mind Research Network, Albuquerque, NM, USA, [8] Department of Psychiatry, Yale University, New Haven, CT, USA, [9] Department of Radiology, Huaxi MR Research Center, West China Hospital of Sichuan University, Chengdu, China

To investigate whether aberrant interactions between brain structure and function present similarly or differently across probands with psychotic illnesses [schizophrenia (SZ), schizoaffective disorder (SAD), and bipolar I disorder with psychosis (BP)] and whether these deficits are shared with their first-degree non-psychotic relatives. A total of 1199 subjects were assessed, including 220 SZ, 147 SAD, 180 psychotic BP, 150 first-degree relatives of SZ, 126 SAD relatives, 134 BP relatives, and 242 healthy controls (1). All subjects underwent structural MRI (sMRI) and resting-state functional MRI (rs-fMRI) scanning. Joint-independent component analysis (jICA) was used to fuse sMRI gray matter and rs-fMRI amplitude of low-frequency fluctuations data to identify the relationship between the two modalities. jICA revealed two significantly fused components. The association between functional brain alteration in a prefrontal–striatal–thalamic–cerebellar network and structural abnormalities in the default mode network was found to be common across psychotic diagnoses and correlated with cognitive function, social function, and schizo-bipolar scale scores. The fused alteration in the temporal lobe was unique to SZ and SAD. The above effects were not seen in any relative group (including those with cluster-A personality). Using a multivariate-fused approach involving two widely used imaging markers, we demonstrate both shared and distinct biological traits across the psychosis spectrum. Furthermore, our results suggest that the above traits are psychosis biomarkers rather than endophenotypes.

Keywords: schizophrenia, schizoaffective, bipolar, relatives, multimodal neuroimaging, joint-independent component analysis

OPEN ACCESS

Edited by:
Dorota Frydecka, Wroclaw Medical University, Poland

Reviewed by:
Giacomo Salvadore, Janssen Research and Development, USA
André Schmidt, King's College London, UK

***Correspondence:**
Shashwath A. Meda
shashwath.meda@hhchealth.org

Specialty section:
This article was submitted to Affective Disorders and Psychosomatic Research, a section of the journal Frontiers in Psychiatry

Received: *19 August 2015*
Accepted: *27 November 2015*
Published: *21 December 2015*

Citation:
Wang Z, Meda SA, Keshavan MS, Tamminga CA, Sweeney JA, Clementz BA, Schretlen DJ, Calhoun VD, Lui S and Pearlson GD (2015) Large-Scale Fusion of Gray Matter and Resting-State Functional MRI Reveals Common and Distinct Biological Markers across the Psychosis Spectrum in the B-SNIP Cohort. Front. Psychiatry 6:174. doi: 10.3389/fpsyt.2015.00174

INTRODUCTION

Whether schizophrenia (SZ), schizoaffective disorder (SAD), and psychotic bipolar disorder are distinct illnesses or represent a continuum continues to be debated (2–4). There is overlap among clinical symptoms (5), cognitive functional deficits (6), and disease risk genes (7) among these disorders (8) that challenge traditional diagnostic categories. Clarifying similarities and differences in anatomical and functional deficits among psychotic probands may contribute to the better understanding of the mechanisms underlying psychotic disorders. The above disorders are highly heritable (9, 10), and illness-related genes associated with the abnormalities in brain structure and function (11) may also be present in their unaffected relatives. Thus, shared abnormalities between probands and unaffected relatives can serve as endophenotypes, which may provide biological genetic substrates for improved diagnostic classification (12), and ultimately may lead to better, more focused treatments.

Psychotic illnesses are widely assumed to be brain disorders characterized by distributed cerebral dysconnectivity across large-scale neural networks. Resting-state networks reflect correlated spontaneous fluctuations in brain regional activity at rest (13) and show a similar correspondence to task-related networks that control brain action and cognition (14). A recent resting-state functional MRI (rs-fMRI) study reported that SZ, SAD, and psychotic bipolar disorder share disruptions within the fronto-parietal control network (7). Both default mode network (DMN) and prefrontal–thalamic–cerebellar network connectivity have been reported to be abnormal in probands with SZ and bipolar disorder (15, 16) and between probands and relatives with SZ (17–19). Lui et al. (20) compared resting-state functional network connectivity between SZ and psychotic bipolar probands and their unaffected first-degree relatives and found probands with SZ and psychotic bipolar shared deficits in striatal–thalamic–cortical network as well as bipolar relatives. Independent structural MRI (sMRI) studies reveal both common and unique regional gray matter (GM) abnormalities across psychotic probands (21–24). Ivleva et al. (24) reported that SZ, SAD, psychotic bipolar disorder probands, and their relatives with psychosis showed overlapping GM deficits throughout the neocortex as a psychosis endophenotype. Collectively, overlaps and differences in both functional and structural networks across psychosis probands and their relatives have been identified, but no studies to date have examined both structural and functional deficits together. Brain regions are highly interconnected and local changes in brain structure may result in altered brain activity in distant regions (25, 26). Inter-regional correlations of GM volume may reflect changed inter-regional functional connectivity (27). Thus, examining abnormalities in structure and function together may help better characterize illness-related features and provide more information than each measure independently.

Joint-independent component analysis (jICA), a data-driven feature-based approach, enables joint analysis of different data types, for example, relationships between brain function and structure (28). In the present study, we utilized two commonly employed techniques to quantify anatomy and function. Anatomical data were indexed by GM volumes obtained through voxel-based morphometry (VBM), while resting-state function was measured using amplitude of low-frequency fluctuations (ALFF) (0.01–0.08 Hz) of the blood oxygen level dependent. ALFF measures, particularly in the 0.01–0.08 Hz frequency range have been demonstrated to be physiologically relevant and related to neuronal fluctuations in brain GM in resting state (29, 30). In the current study, we utilized the joint approach to integrate GM and ALFF, to investigate joint structure–function anomalies across the SZ-psychotic bipolar disorder spectrum using data from the large-scale multi-site bipolar-schizophrenia network on intermediate phenotypes (B-SNIP) psychosis study (31). Our aims were to (1) detect whether aberrancies detected by fusing rs-fMRI and sMRI would be specific to SZ, SAD, or bipolar I disorder with psychosis (BP) or shared by these psychotic disorders relative to healthy controls; (2) investigate whether these abnormalities across two modalities would be shared by probands and their non-psychotic relatives, suggesting that they may represent endophenotypes across the psychosis dimension.

MATERIALS AND METHODS

Participants

A total of 1199 subjects (passing quality control) were used for the current analysis. Subjects were drawn from the B-SNIP study from six sites, including 220 SZ, 180 psychotic BP, 147 SAD, 150 first-degree relatives of SZ, 134 first-degree relatives of psychotic BP, 126 first-degree relatives of SAD, and 242 healthy controls. The details of characteristics of the B-SNIP clinical population are described in Ref. (31). All participants provided written informed consent approved separately by institutional review boards of individual sites after a complete explanation of the study. All probands and relatives were diagnosed using the Structured Clinical Interview for DSM-IV Axis I Disorder, Patient Edition (SCID-I/P) (32). Relatives were also diagnosed with the structured interview for DSM-IV personality (SIDP-IV) (33) for axis-II diagnoses. Relatives meeting the criteria for axis I proband-like psychotic disorders ($N = 64$) were classified to the corresponding proband groups and those with no axis I or no lifetime psychotic diagnoses were included in the non-psychotic relative groups. In addition, relatives without a psychotic disorder were administered the SIDP-IV (34) and were considered to have elevated psychosis spectrum personality traits if meeting full or within one criteria of Cluster-A (psychosis spectrum; $N = 63$) Axis-II diagnosis. Healthy controls were evaluated using the SCID Non-Patient Edition to confirm lifetime absence of Axis I illness or a family history of SZ-bipolar spectrum disorders. All probands were assessed with positive and negative syndrome scale (PANSS) (35), Montgomery–Åsberg depression rating scale (MADRS) (36), Young Mania Rating Scale (YMRS) (37), and schizo-bipolar scale (SBS) (5). Additionally, all subjects were assessed with brief assessment of cognition in schizophrenia (BACS) (38) and the Birchwood social functioning scale (SFS) (39).

The demographic and clinical characteristics of study sample are outlined in **Table 1**, and details are described in the previous B-SNIP papers (24, 31). Medication data are listed in Table S2 in Supplementary Material.

TABLE 1 | Demographic and clinical characteristics of the study sample.

Variable[a]	Schizophrenia probands (n =220)		Schizoaffective disorder probands (n =147)		Psychotic bipolar probands (n =180)		Relatives of schizophrenia (n =150)		Relatives of schizoaffective disorder (n =126)		Relatives of psychotic bipolar (n =134)		Healthy controls (n =242)		Statistic[c]	
	N	%	*N*	%	*N*	%	*N*	%	*N*	%	*N*	%	*N*	%	χ^2	*p*
Male gender	145	65.91	66	44.90	58	32.22	49	32.67	40	31.75	49	36.57	103	42.56	71.27	2×10^{-13}
	Mean	**SD**	**Mean**	**SD**	**Mean**	**SD**	**Mean**	**SD**	**Mean**	**SD**	**Mean**	**SD**	**Mean**	**SD**	***F***	***p***
Age (years)	35.15	12.31	35.08	12.01	36.94	13.04	43.33	15.55	41.01	16.14	40.59	16.13	38.14	12.65	7.72	4×10^{-8}
PANSS																
Positive	16.91	5.42	18.12	5.32	12.77	4.38	–	–	–	–	–	–	–	–	50.47	1×10^{-22}
Negative	16.27	5.93	15.49	4.95	11.79	3.61	–	–	–	–	–	–	–	–	40.96	3×10^{-17}
General	32.02	8.72	34.80	9.00	28.60	8.04	–	–	–	–	–	–	–	–	20.57	3×10^{-9}
Total	65.20	16.78	68.41	16.28	53.17	13.48	–	–	–	–	–	–	–	–	43.74	3×10^{-18}
MADRS	8.90	7.93	14.31	10.26	10.51	8.99	–	–	–	–	–	–	–	–	15.76	2×10^{-7}
YMRS	5.76	5.79	7.69	6.48	5.69	6.46	–	–	–	–	–	–	–	–	5.22	0.006
SBS	7.79	1.36	5.01	1.60	1.35	1.24	–	–	–	–	–	–	–	–	1006.21	2×10^{-178}
BACS[b] (z)																
Verbal memory	−1.14	1.32	−1.04	1.39	−0.44	1.28	−0.08	1.09	−0.46	1.26	−0.13	1.07	−0.04	1.08	23.13	8×10^{-26}
Token motor	−1.33	1.18	−1.36	1.17	−0.95	1.24	−0.33	1.16	−0.24	1.03	−0.31	1.07	0.02	1.12	39.24	3×10^{-43}
Digit sequencing	−1.26	1.20	−0.94	1.28	−0.51	1.11	−0.38	1.14	-0.27	1.15	−0.03	1.11	−0.06	1.12	26.71	8×10^{-30}
Verbal fluency	−0.76	1.15	−0.50	1.27	−0.20	1.23	−0.93	1.08	0.02	1.20	0.07	1.07	0.14	1.05	14.20	1×10^{-15}
Symbol coding	−1.41	1.10	−1.37	1.18	−0.87	1.01	−0.37	1.08	−0.39	1.10	−0.07	1.04	−0.00	1.01	49.42	1×10^{-53}
Tower of London	−0.87	1.39	−0.70	1.30	−0.28	1.10	−0.19	1.08	−0.18	1.27	0.11	0.85	0.02	1.17	15.80	2×10^{-17}
Composite score	−1.79	1.34	−1.54	1.37	−0.87	1.24	−0.38	1.19	−0.40	1.25	−0.09	1.11	0.02	1.17	54.99	3×10^{-59}
SFS	123.27	23.13	119.28	24.42	134.10	22.77	151.03	18.23	144.64	21.89	151.42	21.60	156.09	15.94	68.31	2×10^{-70}

[a]*PANSS, positive and negative syndrome scale; MRADS, Montgomery–Åsberg depression rating scale; YMRS, Young Mania Rating Scale; SBS, schizo-bipolar scale; BACS, brief assessment of cognition in schizophrenia; SFS, Birchwood social functioning scale.*

[b]*z-Scores are calculated using the overall means and standard deviations of all healthy controls and corrected with age and sex.*

[c]*Post hoc statistic are presented as follows: age: SADR, SZR > HC; SZR, BPR, SADR > BP; HC, BPR, SADR, SZR > SZ; BPR, SADR, SZR > SAD. PANSS_Positive: SZ > BP; SAD > SZ, BP; PANSS_Negative: SZ > BP, SAD; SAD > BP; PANSS General: SAD > SZ > BP. MADRS: BP > HC; SZ > HC; SAD > all groups. YMRS: BP > HC; SZ > HC; SAD > all groups. SBS: SZ > BP, SAD; SAD > BP. BACS Verbal memory: BP > SZ, SAD; HC > SZ, SAD, BP; SADR > BP; SZR, BPR, HC > SADR; BACS token motor: BP > SZ, SAD; HC > SZ, SAD, BP; HC, SADR > SZR, BPR; BACS digit sequencing: BP > SAD > SZ; HC > SZ, SAD, BP, SZR; BACS verbal fluency: BP > SAD > SZ; HC > SZ, SAD, BP; BACS symbol coding: BP > SZ, SAD; HC > SZ, SAD, BP, SZR, SDAR; BACS tower of London: BP > SZ, SAD; HC > SZ, SAD, BP; BACS composite Score: BP > SZ, SAD; HC > SZ, SAD, BP; SADR > BP; SZR, BPR, HC > SADR.SFS: BP, SZR, BPR, SADR, HC > SZ, SAD; BP > SAD, SZ; SZR, BPR, SADR, HC > BP; SZR, BPR > SADR; HC > BP, SAD, SZ, SZR, SADR.*

MRI Data Acquisition and Preprocessing

Structural and functional MRI scans were acquired on 3-T scanners at each site (Scanning platforms and platforms parameters are listed in Table S1 in Supplementary Material). Structural and functional images were collected during the same scan session. Foam pads and ear plugs were used to minimize head motion and scanner noise. All the subjects were instructed to keep their eyes fixated on a crosshair, not to think about anything in particular and to move as little as possible.

Voxel-Based Morphometry

Voxel-based morphometry analyses of structural images were performed using the VBM8 toolbox[1] as implemented in SPM8. T1-weighted images were bias-corrected and segmented into GM, white matter (WM), and cerebrospinal fluid (CSF) by "New Segment" using a customized template, which was constructed from our 1199 study samples by DARTEL in SPM8 (40). The segmented images were normalized to Montreal Neurological Institute (MNI) space (41) using the DARTEL template and resampled to 1.5 mm × 1.5 mm × 1.5 mm voxels. In the final step, the segmented normalized images were spatially smoothed with an 8 mm × 8 mm × 8 mm full width at half maximum Gaussian kernel.

Amplitude of Low-Frequency Fluctuations

Functional image preprocessing was carried out using data processing assistant for resting-state fMRI (DPARSF), version 2.3 (42), implemented in the MATLAB toolbox (Mathworks, Inc.). The first 9 s of each subject data were discarded before slice timing and head motion correction were performed. Then, the individual structural T1 image was coregistered to the mean functional image after motion correction. Subjects with head motion >3.0 mm of maximal translation in any direction or 3.0° of maximal rotation were excluded from further analysis. In addition, six motion parameters, CSF, and WM signals were used as nuisance covariates to reduce effects of head motion and non-neuronal BOLD fluctuations. Images were then DARTEL normalized to MNI space and resampled to 3 mm × 3 mm × 3 mm voxels. Subsequently, the time series were band-pass filtered (0.01–0.08 Hz) and linear trends removed. Then, the preprocessed time series were transformed to the frequency domain using fast Fourier transform, and power spectra obtained. Because the power of a given frequency is proportional to the square of the amplitude of this frequency component of the original time series in the time domain, the square root was calculated at each frequency of the power spectrum and the averaged square root was obtained across 0.01–0.08 Hz at each voxel. This averaged square root was taken as the ALFF. For standardization purpose, the ALFF of each voxel was divided by the global mean ALFF value. Finally, all images were spatially smoothed with an 8 mm × 8 mm × 8 mm full width at half maximum Gaussian kernel.

[1] http://dbm.neuro.uni-jena.de/vbm

Joint-Independent Component Analysis

Joint-independent component analysis is a second-level fMRI analysis method that assumes two or more features (modalities) share the same mixing matrix and maximizes the independence among joint components. ICA is performed on the horizontally concatenated feature sets (along voxels in structure–function in this case), thus uncovering patterns of data that commonly fluctuate or are connected across both modalities (see Figure S1 in Supplementary Material). It is suitable for examining a common modulation across subjects among modalities and has been applied to link a variety of feature sets in the past (43, 44). jICA (28, 45) assumes a model $\chi = AS$ where joint-independent sources (S) are linearly mixed by a common mixing parameter (A) to generate the observations data matrix (χ). In this case, we use ICA analysis algorithms to form the overall data matrix $\chi = [\chi^{GM}, \chi^{ALFF}]$ and derive spatially independent joint sources $S = [S^{GM}, S^{ALFF}]$ along with their shared mixing parameter (A), which are presented as loading parameters for each subject. A total of 22 independent components were estimated according to minimum description length criteria (46) using the Group ICA of fMRI Toolbox (GIFT).[2] The jICA was performed using the Fusion ICA Toolbox.[3] First, the preprocessed ALFF and GM images were normalized to have the same average sum of squares to ensure that units were shared between data types. Normalization was performed on group level, so covariations among subjects were preserved. Then, the ALFF and GM data were modeled by matching the sums of squares across modalities and combined into a single data matrix, used to identify the common mixing matrix parameters using the infomax algorithm (47) shared by spatially independent joint source images (ALFF and GM images). The complete details of the method were as reported in Ref. (28).

Statistical Analysis

A one-way analysis of variance (ANOVA) and chi-square test were carried out for demographic and clinical variables. The effects of age, sex, and site were regressed out using linear regression, and residuals of loading parameters of the independent components were compared across probands, relatives, and HC using ANOVA. Independent components showing significant main effect of group difference after Bonferroni correction were further evaluated using *post hoc* pair-wise group comparisons. A false discovery rate (FDR) correction for multiple comparisons was applied to *post hoc* tests. To assess whether the estimated ICA joint sources were associated with clinical symptoms, cognitive, or general socio-functioning, we derived associations between the residuals of the independent components and PANSS, MADRS, YMRS, BACS, and SFS scores across all available subjects. For the above association analyses, we added group as an additional covariate to covary any baseline group differences in cognition and social function.

In addition, relative risk (48) of joint structural–functional abnormalities presented by the independent components was calculated as the ratio of percentage of relatives classified as

[2] http://mialab.mrn.org/software/gift, version 2.0a

[3] http://mialab.mrn.org/software/fit, version 1.2c

"affected" based on a threshold of 2 SD above the control mean to the percentage of healthy controls designated as "affected." A chi-square was used to test for significance of relative risk in relatives compared with HC.

Furthermore, we used an ANCOVA model to detect the main effect of site across healthy controls and the effect of diagnosis-by-site across all groups separately. The above analyses were performed using SPSS v17.0 (Statistical Package for the Social Sciences, IBM, Chicago, IL, USA).

RESULTS

Of the 22 components estimated from the data, only network pair 6 (IC6) ($F = 9.62$; $p = 7 \times 10^{-5}$) and IC15 ($F = 17.79$; $p = 2 \times 10^{-8}$) showed a group main effects after Bonferroni correction. Talairach coordinates for the regions of IC15 and IC6 at a threshold of $|Z| > 2.5$ are summarized in **Tables 2** and **3**. The ALFF/GM maps of IC15 and IC6 are shown in **Figure 1**. As part of the output, jICA also produces loading parameters for each component pair that reflects the component's influence at the subject level (49). This is further used to assess the between-subject differences in sMRI–fMRI association. *Post hoc* tests revealed loading parameters of IC6 were higher both in probands with SZ ($p = 0.024$) and SAD ($p = 0.012$) in relative to healthy controls. For IC 15, loading parameters were lower in probands with SZ ($p = 0.012$), SAD ($p = 0.024$), and BP ($p = 0.036$) relative to healthy controls separately. Contrasts revealed no effect of relatives and healthy controls in either IC6 or IC15. The mean standardized residual of loading parameters are shown in **Figure 2**. All *posthoc* measures were corrected using the FDR method (for reference).

We correlated the loading parameters of both ICs with the PANSS, MADRS, YMRS, BACS, SBS, and SFS scores for all available subjects. While, loading parameters of IC6 showed no correlation with any of the above scores. Loading parameters of IC15 were positively correlated with the BACS composite scores, BACS symbol coding scores, and BACS tower of London scores after FDR correction (**Table 4**).

TABLE 2 | Talairach coordinates for significant regions of component 15.

Region	BA	Left/right volume (cc)	Left/right Z_{max} (*x*, *y*, *z*)
IC15_ALFF			
CONTROLS > PROBANDS			
Lingual gyrus	17, 18	2.3/1.4	6.9 (−3, −91, −11)/6.7 (6, −88, −11)
Thalamus	NA	1.6/2.1	4.5 (−9, −5, 11)/4.1 (6, −5, 11)
Culmen	NA	1.7/1.5	3.2 (−18, −30, −16)/3.5 (0, −39, −21)
Declive	NA	1.1/1.0	3.6 (−18, −88, −18)/3.5 (3, −79, −11)
Superior temporal gyrus	38	0.0/1.9	NA/4.0 (36, 8, −21)
Caudate	NA	0.6/1.0	5.0 (−9, 4, 14)/4.5 (9, 6, 11)
Superior frontal gyrus	6, 8, 10	1.3/0.0	2.8 (−30, 61, −3)/NA
Rectal gyrus	11	0.6/0.5	2.7 (−3, 34, −22)/2.5 (3, 37, −25)
Cuneus	17, 18, 19	0.7/0.0	3.3 (−3, −93, 0)/NA
Fusiform gyrus	18	0.6/0.0	5.0 (−21, −91, −13)/NA
Inferior occipital gyrus	17, 18	0.6/0.0	4.1 (−30, −88, −13)/NA
Precuneus	7	0.5/0.0	3.3 (−3, −76, 45)/NA
Anterior cingulate	25	0.5/0.0	3.5 (0, 2, −10)/NA
PROBANDS > CONTROLS			
Inferior frontal gyrus	13, 47	1.2/0.8	3.2 (−39, 11, −13)/2.8 (24, 11, −16)
Middle temporal gyrus	21, 38	1.3/0.3	3.0 (−39, 4, −30)/2.4 (48, 4, −30)
Middle occipital gyrus	18, 37	0.0/0.9	NA/2.5 (33, −76, −9)
Superior temporal gyrus	22, 38	0.6/0.0	2.6 (−39, 7, −28)/NA
Cuneus	17, 18	0.0/0.6	NA/2.6 (6, −84, 12)
Transverse temporal gyrus	41, 42	0.0/0.5	NA/3.2 (62, −14, 12)
IC15_GM			
CONTROLS > PROBANDS			
Cingulate gyrus	24, 31, 32	7.0/6.4	3.6 (−4, 25, 28)/3.4 (6, 28, 28)
Medial frontal gyrus	6, 8, 9, 10, 11, 32	5.9/5.6	3.2 (−7, 46, 12)/3.6 (4, 42, 15)
Anterior cingulate	10, 24, 32	4.1/4.6	3.5 (−4, 43, 13)/3.8 (7, 36, 19)
Paracentral lobule	5, 6, 31	1.1/1.0	2.9 (−3, −11, 43)/3.0 (9, −25, 44)
Precuneus	7, 31	1.3/0.6	3.0 (−13, −62, 22)/2.7 (15, −57, 24)
Posterior cingulate	30	0.8/0.7	3.2 (−13, −56, 17)/2.7 (15, −53, 15)
Middle frontal gyrus	9	0.0/0.8	NA/3.0 (40, 10, 30)
PROBANDS > CONTROLS			
Lingual gyrus	17, 18	1.7/1.3	3.1 (0, −86, −7)/3.0 (3, −88, −4)
Fusiform gyrus	19, 20, 37	0.3/0.7	2.3 (−52, −66, −12)/2.5 (52, −63, −13)

NA = not applicable.

TABLE 3 | Talairach coordinates for significant regions of component 6.

Region	BA	Left/right volume (cc)	Left/right Z_{max} (x, y, z)
IC6_ALFF			
PROBANDS > CONTROLS			
Uncus	20, 28, 34, 36	5.1/4.9	8.6 (−33, −1, −28)/8.9 (33, −4, −28)
Superior temporal gyrus	38	3.4/4.4	7.8 (−33, 5, −23)/7.9 (39, 2, −20)
Middle temporal gyrus	20, 21, 38	2.6/2.9	7.6 (−39, 2, −28)/10.5 (39, −4, −28)
Parahippocampal gyrus	34, 35	2.6/2.5	8.1 (−33, −4, −20)/9.4 (36, −1, −20)
Inferior temporal gyrus	20	1.9/2.7	5.2 (−45, −4, −28)/8.4 (42, −7, −27)
Fusiform gyrus	20	0.5/0.5	4.1 (−39, −13, −25)/6.9 (42, −10, −25)
IC6_GM			
PROBANDS > CONTROLS			
Fusiform gyrus	20, 36, 37	1.2/1.1	3.9 (−42, −17, −24)/4.2 (42, −16, −24)
Superior temporal gyrus	13, 22, 38, 39, 41	0.8/1.0	3.3 (−27, 15, −30)/3.4 (49, −44, 19)
Middle frontal gyrus	6, 9, 10, 46	0.4/1.2	2.7 (−37, 37, 11)/3.9 (40, 13, 27)
Precuneus	7, 31	1.1/0.2	3.7 (−13, −69, 26)/2.1 (19, −60, 28)
Uncus	20, 28, 36, 38	1.0/0.3	4.1 (−19, 3, −32)/2.8 (22, 9, −27)
Inferior parietal lobule	40	0.8/0.3	3.2 (−43, −34, 39)/4.9 (46, −46, 22)
Inferior frontal gyrus	9, 47	0.3/0.8	2.5 (−39, 34, 13)/3.8 (42, 6, 33)
Inferior temporal gyrus	20, 37	0.0/0.8	NA/3.9 (40, −13, −27)
Precentral gyrus	6, 9, 13, 43	0.0/0.8	NA/3.0 (53, −4, 10)
Supramarginal gyrus	40	0.0/0.8	NA/5.0 (48, −47, 26)
Middle temporal gyrus	37, 39	0.0/0.4	NA/2.7 (34, −76, 18)
CONTROLS > PROBANDS			
Precuneus	7, 31	2.8/2.0	4.6 (−7, −46, 34)/3.2 (4, −48, 33)
Cingulate gyrus	31	1.8/1.6	4.2 (−7, −43, 37)/4.2 (9, −42, 37)
Middle frontal gyrus	9, 10	1.9/1.2	4.6 (−37, 22, 32)/4.5 (37, 25, 32)
Posterior cingulate	23, 30, 31	1.5/0.9	3.8 (−19, −65, 10)/3.5 (18, −64, 10)
Middle temporal gyrus	20, 21	1.7/0.5	2.8 (−56, −41, −9)/2.6 (55, −2, −20)
Lentiform nucleus	*	0.0/1.6	NA/3.2 (19, 14, −3)
Inferior frontal gyrus	45, 47	0.0/1.2	NA/3.4 (50, 22, 10)
Inferior temporal gyrus	20, 21	0.7/0.3	2.5 (−61, −21, −22)/2.6 (58, −23, −15)
Declive	*	0.0/0.7	NA/2.6 (40, −75, −15)
Cuneus	18, 23, 30	0.6/0.0	3.9 (−16, −68, 12)/NA
Precentral gyrus	6, 9	0.3/0.3	5.2 (−37, 21, 36)/3.0 (50, 19, 7)
Lingual gyrus	18, 19	0.4/0.2	3.1 (−16, −51, 5)/2.5 (22, −54, 5)
Parahippocampal gyrus	30	0.3/0.2	2.7 (−22, −52, 5)/3.4 (19, −49, 5)

There was no significant difference between relatives and healthy controls in relative risk of joint structural–functional abnormalities. Main effects of site were observed for both IC6 ($F = 40.63$, $p = 4 \times 10^{-30}$) and IC15 ($F = 9.98$, $p = 1 \times 10^{-8}$). However, more importantly, no diagnosis-by-site interaction was noted.

DISCUSSION

The human brain is connected on a variety of different spatial scales, from synaptic signaling at the cellular level to a more broad systems level containing inter-regional communication across physically distant brain regions. A natural starting point to examine system level architecture is by using traditional "unimodal" techniques. However, it is also possible to apply more advanced statistical techniques to define "cross-modal" brain relationships between disparate measures (e.g., structure and function). In this study, we took this approach to detect common and unique abnormalities in a large psychosis sample by fusing two modalities (rs-fMRI and sMRI) using a jICA approach across the psychotic spectrum (SZ, SAD, and psychotic BP) and to investigate which of those are shared by their unaffected first-degree relatives, suggesting possible endophenotypes. Since multimodal techniques such as joint ICA capture "cross-feature" information simultaneously, they naturally contribute to a different set of information compared to their individual "unimodal" counterparts.

By using a jICA approach, two components showing group differences were identified. Joint loadings computed from IC15 showed significant differences in SZ, SAD, and BP (compared to HC), while IC6 distinguished only SZ and SAD from controls. However, first-degree, non-psychotic relatives showed no common abnormalities with the probands and no significant differences compared to HC. Consistent with this finding, we found that the relative risk estimates for the two components were non-significant. Brain changes in function and structure correlated with certain sub-scales of the BACS inventory, suggesting direction relationships between affected structure–function patterns and cognitive function scores.

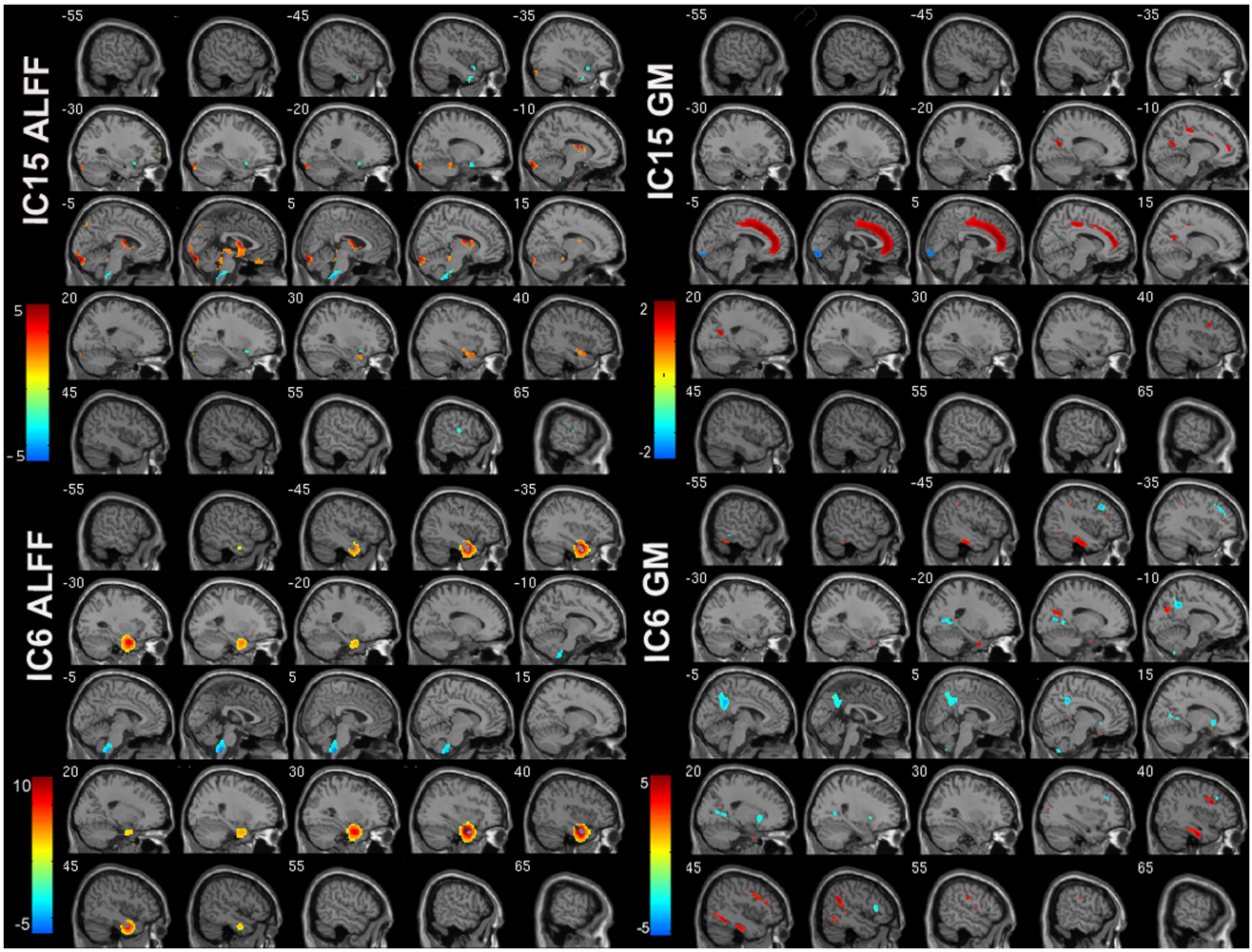

FIGURE 1 | ALFF and GM spatial maps for joint IC6 and IC15. For display, the components were converted to *Z*-values and thresholded at $|Z| > 2.5$.

The IC15-ALFF network encompassed regions, including thalamus, cerebellum, prefrontal cortex, and caudate, which are primarily involved in the prefrontal–striatal–thalamic–cerebellar network that has been implicated in the pathophysiology of both SZ (50, 51) and BP (52), supported by growing evidence (53–59). The prefrontal cortex plays a critical role in executive cognitive control, whereas the striatum and the cerebellum, which are connected with the prefrontal cortex via thalamus (60, 61), are also involved in executive function, working memory, spatial cognition, and language (62). The thalamus not only functions as a nexus to integrate cortical and subcortical activity (63, 64) but is also implicated in processing and integrating sensory information via connections with sensory–motor cortices (65, 66). Remaining brain regions in IC15-ALFF included visual areas, such as lingual gyrus, cuneus, fusiform gyrus, and occipital cortex; and auditory-related areas, such as superior temporal and transverse temporal gyri, which may indicate dysconnectivity between sensory cortices and thalamus in psychosis. Thus, dysfunctions in this network may be associated with abnormal cognition, difficulty in coordinating processing, prioritization, retrieval, and expression of the information associated with psychotic symptoms (51, 67). Consistent with our results, Anticevic et al. (68) documented that thalamic connectivity with prefrontal–striatal–cerebellar regions successfully classified SZ and psychotic bipolar patients, suggesting that this network may be abnormal across diagnoses. Interestingly, IC15 also showed decreased GM in regions that constitute the functional DMN (69), consistent with previous findings in both SZ/SAD and BP that showed reduced GM (24, 70–75). Two regions within IC15 showing increased GM in psychosis probands were lingual gyrus and fusiform gyrus, consistent with previous studies with larger fusiform gyrus in both SZ and BP (76) and larger lingual gyrus in SZ (77) compared with healthy controls. Positive correlation between the loading parameters of IC15 and BACS scores support a link between abnormalities in prefrontal–striatal–thalamic–cerebellar network and DMN and cognitive function, consistent with previous studies (38, 78–84). Interestingly, symbol coding was the most sensitive indicator

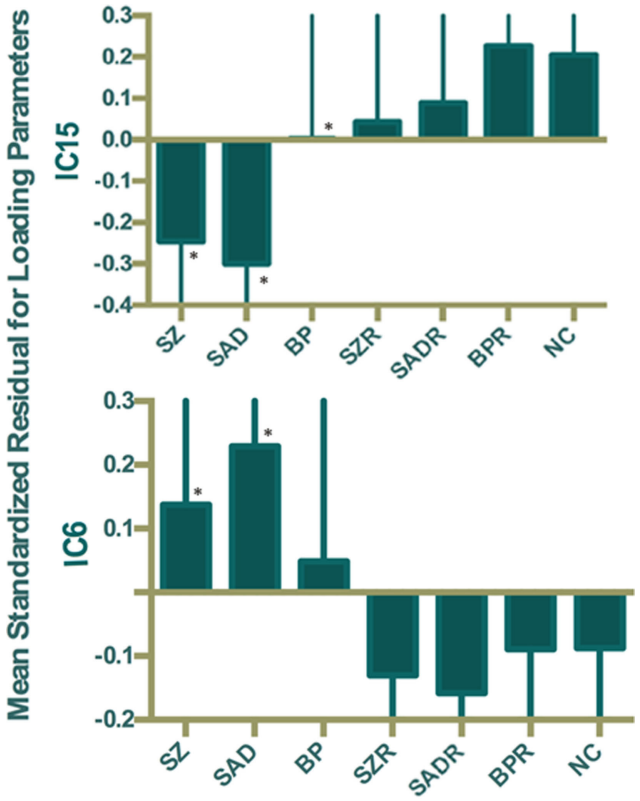

FIGURE 2 | Mean standardized residual of loading parameters for IC15 and IC6, controlling for age, sex, and site. *Individual group had significantly different loading parameters compared to control subjects after false discovery rate (FDR) correction.

TABLE 4 | Significant correlations between IC15 loading parameters and the brief assessment of cognition in schizophrenia adjusted using FDR correction for multiple comparisons.

IC15	BACS (*z*)	*R*	*p**
	Symbol coding	0.175	0.001
	Tower of London	0.157	0.003
	Composite score	0.169	0.001

**FDR corrected.*

of genetic liability for SZ/SAD and performance distinguished psychotic BP from major depression (85).

Among the IC6-ALFF regions, a subset of temporal regions showed higher ALFF in both SZ and SAD in relative to HC and no difference between BP and controls. These results are consistent with previous studies that increased ALFF were found in inferior temporal gyrus, uncus, fusiform gyrus (86), superior temporal gyrus (87), and parahippocampal gyrus (88) in SZ when compared to HC. All these regions overlap with the IC6-GM regions, which suggest that both temporal lobe function and structure are disturbed in SZ and SAD (89, 90). Regions noted as part of IC6-GM have been consistently shown to have reduced GM in SZ compared to HC (91, 92), often in association with psychotic symptoms (93). Another jICA study (28) that combined fMRI (from an auditory oddball task) and sMRI data showed similar brain regions to ours with both increased GM and abnormal activation primarily located in temporal lobe in SZ compared to HC. Furthermore, consistent with our results, Calhoun et al. (94) reported that temporal lobe functional data successfully discriminated HC from SZ during an auditory oddball task, and combined temporal lobe and DMN data in resting-state discriminated between SZ and psychotic BP, consistent with well-studied temporal lobe anomalies in SZ (45).

A natural question is what mechanisms may be responsible for these types of long-distance structural–functional couplings and how functional data in one region might be linked to a different/remotely located functional region or vice versa. One possibility is that the local GM volume in one region affects the quantity of functional output from that region, which in turn has a causal influence on synaptic input arriving at a distal cortical location, thus suggesting a relationship from structure to downstream functional response. Alternatively, the causal direction of the relationship could be reversed, with the amount of functional activity in a region influencing the structural volume of a downstream region, either through excitotoxic or neurotrophic influences. Notably, an excitotoxic downstream effect would be a mechanism by which increased functional activity in one region (if consistently elevated) could lead to decreased structural volume in another region. In all these hypothesized mechanisms, it is possible that the observed structure–function relationship is mediated by intervening regions (either direct or indirect connections). Overall, multiple mechanisms and pathways could lead to a coupling between structural and functional characteristics of the brain. Because these mechanisms are not static, it seems likely that the strength and directionality of structure–function correlations could vary in psychiatric populations, such as SZ, where brain connectivity is compromised in general.

The current subject sample largely overlapped with two previously published studies from our group investigating sMRI and ALFF individually in a more traditional "unimodal" voxel-wise fashion (24, 95). Importantly, these previous studies did not look at connectivity of regions as being presently reported here. Overall, in these previously reported studies, we identified larger structural and functional anomalies in SZ/SAD compared to PBP, consistent with findings from the current jICA approach. However, not all regions reported in the current study overlapped with previous findings. This is not surprising, given that jICA (a) is a purely data-driven (blind) technique, (b) captures data patterns that are linked between multimodal features, and (c) explores connectivity patterns among large-scale networks as opposed to regional effects. The jICA approach is therefore a completely different and novel approach to explore the data compared to traditional voxel-wise/regional methods, as reported previously.

Advantages of our study are the relatively large population with psychosis probands and relatives across the psychosis dimension and we combine two different data type to investigate the abnormalities. Limitations of the study include the potential confounds related to medication and illness state (96).

In summary, this study provides evidence based on a large sample of psychosis probands and relatives that associate between

functional brain alterations (ALFF) in a prefrontal–striatal–thalamic–cerebellar network and structural abnormalities (GM) in DMN are common disturbances across psychotic diagnoses, while the alteration in both function and structure in temporal lobe are unique to SZ and SAD. Our results also suggest that SAD is more similar to SZ across the schizo-bipolar spectrum. Comparisons between relatives and HC reveal that these structural–functional abnormalities may be psychosis biomarkers rather than endophenotypes. Future research investigating associations between different data types, fusing information from different modalities, may provide more clues to uncover the mechanisms of psychotic illnesses, leading to a biologically driven classification and more efficient and ultimately personalized treatment strategies.

FUNDING

The current study was funded and supported by the following grants NIMH MH077851, MH078113, MH077945, MH077852, P20GM103472, and MH077862. MK has received a grant from Sunovion. JS has receives support from Janssen, Takeda, BMS, Roche, and Lilly. GP has been a consultant for Bristol-Meyer Squibb.

SUPPLEMENTARY MATERIAL

The Supplementary Material for this article can be found online at http://journal.frontiersin.org/article/10.3389/fpsyt.2015.00174

REFERENCES

1. Théberge J, Williamson KE, Aoyama N, Drost DJ, Manchanda R, Malla AK, et al. Longitudinal grey-matter and glutamatergic losses in first-episode schizophrenia. *Br J Psychiatry* (2007) **191**(4):325–34. doi:10.1192/bjp.bp.106.033670
2. Berrettini W. Evidence for shared susceptibility in bipolar disorder and schizophrenia *Am J Med Genet C Semin Med Genet* (2003) 1**23C**(1):59–64. doi:10.1002/ajmg.c.20014
3. Lake CR, Hurwitz N. Schizoaffective disorder merges schizophrenia and bipolar disorders as one disease-there is no schizoaffective disorder. *Curr Opin Psychiatry* (2007) **20**(4):365–79. doi:10.1097/YCO.0b013e3281a305ab
4. Craddock N, O'Donovan MC, Owen MJ. Psychosis genetics: modeling the relationship between schizophrenia, bipolar disorder, and mixed (or "schizoaffective") psychoses. *Schizophr Bull* (2009) **35**(3):482–90. doi:10.1093/schbul/sbp020
5. Keshavan MS, Morris DW, Sweeney JA, Pearlson G, Thaker G, Seidman LJ, et al. A dimensional approach to the psychosis spectrum between bipolar disorder and schizophrenia: the schizo-bipolar scale. *Schizophr Res* (2011) **133**(1–3):250–4. doi:10.1016/j.schres.2011.09.005
6. Hill SK, Harris MS, Herbener ES, Pavuluri M, Sweeney JA. Neurocognitive allied phenotypes for schizophrenia and bipolar disorder. *Schizophr Bull* (2008) **34**(4):743–59. doi:10.1093/schbul/sbn027
7. Baker JT, Holmes AJ, Masters GA, Yeo BT, Krienen F, Buckner RL, et al. Disruption of cortical association networks in schizophrenia and psychotic bipolar disorder. *JAMA Psychiatry* (2014) **71**(2):109–18. doi:10.1001/jamapsychiatry.2013.3469
8. Ivleva E, Thaker G, Tamminga CA. Comparing genes and phenomenology in the major psychoses: schizophrenia and bipolar 1 disorder. *Schizophr Bull* (2008) **34**(4):734–42. doi:10.1093/schbul/sbn051
9. Cardno AG, Marshall EJ, Coid B, Macdonald AM, Ribchester TR, Davies NJ, et al. Heritability estimates for psychotic disorders: the Maudsley twin psychosis series. *Arch Gen Psychiatry* (1999) **56**(2):162–8. doi:10.1001/archpsyc.56.2.162
10. McGuffin P, Rijsdijk F, Andrew M, Sham P, Katz R, Cardno A. The heritability of bipolar affective disorder and the genetic relationship to unipolar depression. *Arch Gen Psychiatry* (2003) **60**(5):497–502. doi:10.1001/archpsyc.60.5.497
11. Meda SA, Ruaño G, Windemuth A, O'Neil K, Berwise C, Dunn SM, et al. Multivariate analysis reveals genetic associations of the resting default mode network in psychotic bipolar disorder and schizophrenia. *Proc Natl Acad Sci U S A* (2014) **111**(19):E2066–75. doi:10.1073/pnas.1313093111
12. Gottesman II, Gould TD. The endophenotype concept in psychiatry: etymology and strategic intentions. *Am J Psychiatry* (2003) **160**(4):636–45. doi:10.1176/appi.ajp.160.4.636
13. Smith SM, Vidaurre D, Beckmann CF, Glasser MF, Jenkinson M, Miller KL, et al. Functional connectomics from resting-state fMRI. *Trends Cogn Sci* (2013) **17**(12):666–82. doi:10.1016/j.tics.2013.09.016
14. Smith SM, Fox PT, Miller KL, Glahn DC, Fox PM, Mackay CE, et al. Correspondence of the brain's functional architecture during activation and rest. *Proc Natl Acad Sci U S A* (2009) **106**(31):13040–5. doi:10.1073/pnas.0901846106
15. Ongür D, Lundy M, Greenhouse I, Shinn AK, Menon V, Cohen BM, et al. Default mode network abnormalities in bipolar disorder and schizophrenia. *Psychiatry Res* (2010) **183**(1):59–68. doi:10.1016/j.pscychresns.2010.04.008
16. Calhoun VD, Sui J, Kiehl K, Turner J, Allen E, Pearlson G. Exploring the psychosis functional connectome: aberrant intrinsic networks in schizophrenia and bipolar disorder. *Front Psychiatry* (2012) **2**:75. doi:10.3389/fpsyt.2011.00075
17. Whalley HC, Simonotto E, Flett S, Marshall I, Ebmeier KP, Owens DG, et al. fMRI correlates of state and trait effects in subjects at genetically enhanced risk of schizophrenia. *Brain* (2004) **127**(Pt 3):478–90. doi:10.1093/brain/awh070
18. Whalley HC, Simonotto E, Marshall I, Owens DG, Goddard NH, Johnstone EC, et al. Functional disconnectivity in subjects at high genetic risk of schizophrenia. *Brain* (2005) **128**(Pt 9):2097–108. doi:10.1093/brain/awh556
19. Whitfield-Gabrieli S, Thermenos HW, Milanovic S, Tsuang MT, Faraone SV, McCarley RW, et al. Hyperactivity and hyperconnectivity of the default network in schizophrenia and in first-degree relatives of persons with schizophrenia. *Proc Natl Acad Sci U S A* (2009) **106**(4):1279–84. doi:10.1073/pnas.0809141106
20. Lui S, Yao L, Xiao Y, Keedy SK, Reilly JL, Keefe RS, et al. Resting-state brain function in schizophrenia and psychotic bipolar probands and their first-degree relatives. *Psychol Med* (2015) **45**(1):97–108. doi:10.1017/S003329171400110X
21. McDonald C, Marshall N, Sham PC, Bullmore ET, Schulze K, Chapple B, et al. Regional brain morphometry in patients with schizophrenia or bipolar disorder and their unaffected relatives. *Am J Psychiatry* (2006) **163**(3):478–87. doi:10.1176/appi.ajp.163.3.478
22. Emsell L, McDonald C. The structural neuroimaging of bipolar disorder. *Int Rev Psychiatry* (2009) **21**(4):297–313. doi:10.1080/09540260902962081
23. Ivleva EI, Bidesi AS, Thomas BP, Meda SA, Francis A, Moates AF, et al. Brain gray matter phenotypes across the psychosis dimension. *Psychiatry Res* (2012) **204**(1):13–24. doi:10.1016/j.pscychresns.2012.05.001
24. Ivleva EI, Bidesi AS, Keshavan MS, Pearlson GD, Meda SA, Dodig D, et al. Gray matter volume as an intermediate phenotype for psychosis: bipolar-schizophrenia network on intermediate phenotypes (B-SNIP). *Am J Psychiatry* (2013) **170**(11):1285–96. doi:10.1176/appi.ajp.2013.13010126
25. Mesulam MM. From sensation to cognition. *Brain* (1998) **121**(6):1013–52. doi:10.1093/brain/121.6.1013
26. Skudlarski P, Jagannathan K, Anderson K, Stevens MC, Calhoun VD, Skudlarska BA, et al. Brain connectivity is not only lower but different in schizophrenia: a combined anatomical and functional approach. *Biol Psychiatry* (2010) **68**(1):61–9. doi:10.1016/j.biopsych.2010.03.035
27. Bhojraj TS, Prasad KM, Eack SM, Francis AN, Montrose DM, Keshavan MS. Do inter-regional gray-matter volumetric correlations reflect altered functional connectivity in high-risk offspring of schizophrenia patients? *Schizophr Res* (2010) **118**(1–3):62–8. doi:10.1016/j.schres.2010.01.019
28. Calhoun VD, Adali T, Giuliani NR, Pekar JJ, Kiehl KA, Pearlson GD. Method for multimodal analysis of independent source differences in schizophrenia:

combining gray matter structural and auditory oddball functional data. *Hum Brain Mapp* (2006) **27**(1):47–62. doi:10.1002/hbm.20166
29. Biswal B, Yetkin FZ, Haughton VM, Hyde JS. Functional connectivity in the motor cortex of resting human brain using echo-planar MRI. *Magn Reson Med* (1995) **34**(4):537–41. doi:10.1002/mrm.1910340409
30. Cordes D, Haughton VM, Arfanakis K, Carew JD, Turski PA, Moritz CH, et al. Frequencies contributing to functional connectivity in the cerebral cortex in "resting-state" data. *Am J Neuroradiol* (2001) **22**(7):1326–33.
31. Tamminga CA, Ivleva EI, Keshavan MS, Pearlson GD, Clementz BA, Witte B, et al. Clinical phenotypes of psychosis in the bipolar-schizophrenia network on intermediate phenotypes (B-SNIP). *Am J Psychiatry* (2013) **170**(11):1263–74. doi:10.1176/appi.ajp.2013.12101339
32. First MB, Spitzer RL, Robert L, Gibbon M, Williams Janet BW. *Structured Clinical Interview for DSM-IV Axis I Disorders, Patient Edition, January 1995 FINAL, SCID-I/P Version 2.0*. New York, NY: Biometrics Research Department, New York State Psychiatric Institute (1995).
33. Pfohl B, Blum N, Zimmerman M. *Structured Interview for DSM-IV Personality*. Washington, DC: American Psychiatric Association (1997).
34. Farmer RF, Chapman AL. Evaluation of DSM-IV personality disorder criteria as assessed by the structured clinical interview for DSM-IV personality disorders. *Compr Psychiatry* (2002) **43**(4):285–300. doi:10.1053/comp.2002.33494
35. Kay SR, Fiszbein A, Opler LA. The positive and negative syndrome scale (PANSS) for schizophrenia. *Schizophr Bull* (1987) **13**(2):261. doi:10.1093/schbul/13.2.261
36. Montgomery SA, Asberg M. A new depression scale designed to be sensitive to change. *Br J Psychiatry* (1979) **134**(4):382–9. doi:10.1192/bjp.134.4.382
37. Young RC, Biggs JT, Ziegler VE, Meyer DA. A rating scale for mania: reliability, validity and sensitivity. *Br J Psychiatry* (1978) **133**(5):429–35. doi:10.1192/bjp.133.5.429
38. Keefe RS, Harvey PD, Goldberg TE, Gold JM, Walker TM, Kennel C, et al. Norms and standardization of the brief assessment of cognition in schizophrenia (BACS). *Schizophr Res* (2008) **102**(1–3):108–15. doi:10.1016/S0920-9964(08)70325-6
39. Birchwood M, Smith J, Cochrane R, Wetton S, Copestake S. The social functioning scale. The development and validation of a new scale of social adjustment for use in family intervention programmes with schizophrenic patients. *Br J Psychiatry* (1990) **157**(6):853–9. doi:10.1192/bjp.157.6.853
40. Ashburner J. A fast diffeomorphic image registration algorithm. *Neuroimage* (2007) **38**(1):95–113. doi:10.1016/j.neuroimage.2007.07.007
41. Collins DL, Neelin P, Peters TM, Evans AC. Automatic 3D intersubject registration of MR volumetric data in standardized Talairach space. *J Comput Assist Tomogr* (1994) **18**(2):192–205. doi:10.1097/00004728-199403000-00005
42. Chao-Gan Y, Yu-Feng Z. DPARSF: a MATLAB toolbox for "pipeline" data analysis of resting-state fMRI. *Front Syst Neurosci* (2010) **4**:13. doi:10.3389/fnsys.2010.00013
43. Franco AR, Ling J, Caprihan A, Calhoun VD, Jung RE, Heileman GL, et al. Multimodal and multi-tissue measures of connectivity revealed by joint independent component analysis. *IEEE J Sel Top Signal Process* (2008) **2**(6):986–97. doi:10.1109/JSTSP.2008.2006718
44. Sui J, Adali T, Yu Q, Chen J, Calhoun VD. A review of multivariate methods for multimodal fusion of brain imaging data. *J Neurosci Methods* (2012) **204**(1):68–81. doi:10.1016/j.jneumeth.2011.10.031
45. Calhoun VD, Maciejewski PK, Pearlson GD, Kiehl KA. Temporal lobe and "default" hemodynamic brain modes discriminate between schizophrenia and bipolar disorder. *Hum Brain Mapp* (2008) **29**(11):1265–75. doi:10.1002/hbm.20581
46. Rissanen J. Stochastic complexity and modeling. *Ann Stat* (1986) **4**:1080–100. doi:10.1214/aos/1176350051
47. Bell AJ, Sejnowski TJ. An information-maximization approach to blind separation and blind deconvolution. *Neural Comput* (1995) **7**(6):1129–59. doi:10.1162/neco.1995.7.6.1129
48. Egan MF, Goldberg TE, Gscheidle T, Weirich M, Bigelow LB, Weinberger DR. Relative risk of attention deficits in siblings of patients with schizophrenia. *Am J Psychiatry* (2000) **157**(8):1309–16. doi:10.1176/appi.ajp.157.8.1309
49. Calhoun VD, Adali T, Pearlson GD, Pekar JJ. A method for making group inferences from functional MRI data using independent component analysis. *Hum Brain Mapp* (2001) **14**(3):140–51. doi:10.1002/hbm.1048
50. Andreasen NC, O'Leary DS, Cizadlo T, Arndt S, Rezai K, Ponto LL, et al. Schizophrenia and cognitive dysmetria: a positron-emission tomography study of dysfunctional prefrontal-thalamic-cerebellar circuitry. *Proc Natl Acad Sci U S A* (1996) **93**(18):9985–90. doi:10.1073/pnas.93.18.9985
51. Andreasen NC, Paradiso S, O'Leary DS. "Cognitive dysmetria" as an integrative theory of schizophrenia. *Schizophr Bull* (1998) **24**(2):203–18. doi:10.1093/oxfordjournals.schbul.a033321
52. Strakowski SM, Delbello MP, Adler CM. The functional neuroanatomy of bipolar disorder: a review of neuroimaging findings. *Mol Psychiatry* (2005) **10**(1):105–16. doi:10.1038/sj.mp.4001585
53. Wiser AK, Andreasen NC, O'Leary DS, Watkins GL, Boles Ponto LL, Hichwa RD. Dysfunctional cortico-cerebellar circuits cause 'cognitive dysmetria' in schizophrenia. *Neuroreport* (1998) **9**(8):1895–9. doi:10.1097/00001756-199806010-00042
54. Soares JC. Can brain-imaging studies provide a 'mood stabilizer signature?'. *Mol Psychiatry* (2001) **7**:S64–70. doi:10.1038/sj.mp.4001020
55. Blumberg HP, Martin A, Kaufman J, Leung HC, Skudlarski P, Lacadie C, et al. Frontostriatal abnormalities in adolescents with bipolar disorder: preliminary observations from functional MRI. *Am J Psychiatry* (2003) **160**(7):1345–7. doi:10.1176/appi.ajp.160.7.1345
56. Camchong J, Dyckman KA, Chapman CE, Yanasak NE, McDowell JE. Basal ganglia-thalamocortical circuitry disruptions in schizophrenia during delayed response tasks. *Biol Psychiatry* (2006) **60**(3):235–41. doi:10.1016/j.biopsych.2005.11.014
57. Bor J, Brunelin J, Sappey-Marinier D, Ibarrola D, d'Amato T, Suaud-Chagny MF, et al. Thalamus abnormalities during working memory in schizophrenia. An fMRI study. *Schizophr Res* (2011) **125**(1):49–53. doi:10.1016/j.schres.2010.10.018
58. Marenco S, Stein JL, Savostyanova AA, Sambataro F, Tan HY, Goldman AL, et al. Investigation of anatomical thalamo-cortical connectivity and FMRI activation in schizophrenia. *Neuropsychopharmacology* (2012) **37**(2):499–507. doi:10.1038/npp.2011.215
59. Quidé Y, Morris RW, Shepherd AM, Rowland JE, Green MJ. Task-related fronto-striatal functional connectivity during working memory performance in schizophrenia. *Schizophr Res* (2013) **150**(2–3):468–75. doi:10.1016/j.schres.2013.08.009
60. Middleton FA, Strick PL. Anatomical evidence for cerebellar and basal ganglia involvement in higher cognitive function. *Science* (1994) **266**(5184):458–61. doi:10.1126/science.7939688
61. Middleton FA, Strick PL. Basal ganglia and cerebellar loops: motor and cognitive circuits. *Brain Res Rev* (2000) **31**(2):236–50. doi:10.1016/S0165-0173(99)00040-5
62. Schmahmann JD, Sherman JC. The cerebellar cognitive affective syndrome. *Brain* (1998) **121**(4):561–79. doi:10.1093/brain/121.4.561
63. Cummings JL. Frontal-subcortical circuits and human behavior. *Arch Neurol* (1993) **50**(8):873–80. doi:10.1001/archneur.1993.00540080076020
64. Ramnani N. The primate cortico-cerebellar system: anatomy and function. *Nat Rev Neurosci* (2006) **7**(7):511–22. doi:10.1038/nrn1953
65. Geyer MA, Krebs-Thomson K, Braff DL, Swerdlow NR. Pharmacological studies of prepulse inhibition models of sensorimotor gating deficits in schizophrenia: a decade in review. *Psychopharmacology* (2001) **156**(2–3):117–54. doi:10.1007/s002130100811
66. Turetsky BI, Calkins ME, Light GA, Olincy A, Radant AD, Swerdlow NR. Neurophysiological endophenotypes of schizophrenia: the viability of selected candidate measures. *Schizophr Bull* (2007) **33**(1):69–94. doi:10.1093/schbul/sbl060
67. Damaraju E, Allen EA, Belger A, Ford JM, McEwen S, Mathalon DH, et al. Dynamic functional connectivity analysis reveals transient states of dysconnectivity in schizophrenia. *Neuroimage Clin* (2014) **5**:298–308. doi:10.1016/j.nicl.2014.07.003
68. Anticevic A, Cole MW, Repovs G, Murray JD, Brumbaugh MS, Winkler AM, et al. Characterizing thalamo-cortical disturbances in schizophrenia and bipolar illness. *Cereb Cortex* (2013) **24**(12):3116–30. doi:10.1093/cercor/bht165
69. Buckner RL, Andrews-Hanna JR, Schacter DL. The brain's default network: anatomy, function, and relevance to disease. *Ann N Y Acad Sci* (2008) **1124**:1–38. doi:10.1196/annals.1440.011
70. Farrow TF, Whitford TJ, Williams LM, Gomes L, Harris AW. Diagnosis-related regional gray matter loss over two years in first episode schizophrenia

and bipolar disorder. *Biol Psychiatry* (2005) **58**(9):713–23. doi:10.1016/j.biopsych.2005.04.033
71. Bora E, Fornito A, Yücel M, Pantelis C. Voxelwise meta-analysis of gray matter abnormalities in bipolar disorder. *Biol Psychiatry* (2010) **67**(11):1097–105. doi:10.1016/j.biopsych.2010.01.020
72. Ellison-Wright I, Bullmore E. Anatomy of bipolar disorder and schizophrenia: a meta-analysis. *Schizophr Res* (2010) **117**(1):1–12. doi:10.1016/j.schres.2009.12.022
73. Venkatasubramanian G. Neuroanatomical correlates of psychopathology in antipsychotic-naive schizophrenia. *Indian J Psychiatry* (2010) **52**(1):28–36. doi:10.4103/0019-5545.74304
74. Yu K, Cheung C, Leung M, Li Q, Chua S, McAlonan G. Are bipolar disorder and schizophrenia neuroanatomically distinct? An anatomical likelihood meta-analysis. *Front Hum Neurosci* (2010) **4**:189. doi:10.3389/fnhum.2010.00189
75. Bora E, Pantelis C. Structural trait markers of bipolar disorder: disruption of white matter integrity and localized gray matter abnormalities in anterior fronto-limbic regions. *Biol Psychiatry* (2011) **69**(4):299–300. doi:10.1016/j.biopsych.2010.12.020
76. Anderson D, Ardekani BA, Burdick KE, Robinson DG, John M, Malhotra AK, et al. Overlapping and distinct gray and white matter abnormalities in schizophrenia and bipolar I disorder. *Bipolar Disord* (2013) **15**(6):680–93. doi:10.1111/bdi.12096
77. Mané A, Falcon C, Mateos JJ, Fernandez-Egea E, Horga G, Lomeña F, et al. Progressive gray matter changes in first episode schizophrenia: a 4-year longitudinal magnetic resonance study using VBM. *Schizophr Res* (2009) **114**(1–3):136–43. doi:10.1016/j.schres.2009.07.014
78. Owen AM, Doyon J, Petrides M, Evans AC. Planning and spatial working memory: a positron emission tomography study in humans. *Eur J Neurosci* (1996) **8**(2):353–64. doi:10.1111/j.1460-9568.1996.tb01219.x
79. Beauchamp MH, Dagher A, Aston JA, Doyon J. Dynamic functional changes associated with cognitive skill learning of an adapted version of the Tower of London task. *Neuroimage* (2003) **20**(3):1649–60. doi:10.1016/j.neuroimage.2003.07.003
80. Greicius MD, Krasnow B, Reiss AL, Menon V. Functional connectivity in the resting brain: a network analysis of the default mode hypothesis. *Proc Natl Acad Sci U S A* (2003) **100**(1):253–8. doi:10.1073/pnas.0135058100
81. Broyd SJ, Demanuele C, Debener S, Helps SK, James CJ, Sonuga-Barke EJ. Default-mode brain dysfunction in mental disorders: a systematic review. *Neurosci Biobehav Rev* (2009) **33**(3):279–96. doi:10.1016/j.neubiorev.2008.09.002
82. Forsyth JK, Bolbecker AR, Mehta CS, Klaunig MJ, Steinmetz JE, O'Donnell BF, et al. Cerebellar-dependent eyeblink conditioning deficits in schizophrenia spectrum disorders. *Schizophr Bull* (2012) **38**(4):751–9. doi:10.1093/schbul/sbq148
83. Caletti E, Paoli RA, Fiorentini A, Cigliobianco M, Zugno E, Serati M, et al. Neuropsychology, social cognition and global functioning among bipolar, schizophrenic patients and healthy controls: preliminary data. *Front Hum Neurosci* (2013) **7**:661. doi:10.3389/fnhum.2013.00661
84. Matsuo K, Chen SH, Liu CM, Liu CC, Hwang TJ, Hsieh MH, et al. Stable signatures of schizophrenia in the cortical-subcortical-cerebellar network using fMRI of verbal working memory. *Schizophr Res* (2013) **151**(1–3):133–40. doi:10.1016/j.schres.2013.10.028
85. Glahn DC, Almasy L, Blangero J, Burk GM, Estrada J, Peralta JM, et al. Adjudicating neurocognitive endophenotypes for schizophrenia. *Am J Med Genet B Neuropsychiatr Genet* (2007) **144B**(2):242–9. doi:10.1002/ajmg.b.30446
86. Turner JA, Damaraju E, van Erp TG, Mathalon DH, Ford JM, Voyvodic J, et al. A multi-site resting state fMRI study on the amplitude of low frequency fluctuations in schizophrenia. *Front Neurosci* (2013) **7**:137. doi:10.3389/fnins.2013.00137
87. Lui S, Li T, Deng W, Jiang L, Wu Q, Tang H, et al. Short-term effects of antipsychotic treatment on cerebral function in drug-naive first-episode schizophrenia revealed by "resting state" functional magnetic resonance imaging. *Arch Gen Psychiatry* (2010) **67**(8):783–92. doi:10.1001/archgenpsychiatry.2010.84
88. Hoptman MJ, Zuo XN, Butler PD, Javitt DC, D'Angelo D, Mauro CJ, et al. Amplitude of low-frequency oscillations in schizophrenia: a resting state fMRI study. *Schizophr Res* (2010) **117**(1):13–20. doi:10.1016/j.schres.2009.09.030
89. Pol HEH, Schnack HG, Mandl RC, van Haren NE, Koning H, Collins DL, et al. Focal gray matter density changes in schizophrenia. *Arch Gen Psychiatry* (2001) **58**(12):1118–25. doi:10.1001/archpsyc.58.12.1118
90. McCarley RW, Faux SF, Shenton ME, Nestor PG, Adams J. Event-related potentials in schizophrenia: their biological and clinical correlates and new model of schizophrenic pathophysiology. *Schizophr Res* (1991) **4**(2):209–31. doi:10.1016/0920-9964(91)90034-O
91. Pearlson GD, Barta PE, Powers RE, Menon RR, Richards SS, Aylward EH, et al. Medial and superior temporal gyral volumes and cerebral asymmetry in schizophrenia versus bipolar disorder. *Biol Psychiatry* (1997) **41**(1):1–14. doi:10.1016/S0006-3223(96)00373-3
92. Giuliani NR, Calhoun VD, Pearlson GD, Francis A, Buchanan RW. Voxel-based morphometry versus region of interest: a comparison of two methods for analyzing gray matter differences in schizophrenia. *Schizophr Res* (2005) **74**(2–3):135–47. doi:10.1016/j.schres.2004.08.019
93. Barta PE, Pearlson GD, Powers RE, Richards SS, Tune LE. Auditory hallucinations and smaller superior temporal gyral volume in schizophrenia. *Am J Psychiatry* (1990) **147**(11):1457–62. doi:10.1176/ajp.147.11.1457
94. Calhoun VD, Kiehl KA, Liddle PF, Pearlson GD. Aberrant localization of synchronous hemodynamic activity in auditory cortex reliably characterizes schizophrenia. *Biol Psychiatry* (2004) **55**(8):842–9. doi:10.1016/j.biopsych.2004.01.011
95. Meda SA, Wang Z, Ivleva EI, Poudyal G, Keshavan MS, Tamminga CA, et al. Frequency-specific neural signatures of spontaneous low-frequency resting state fluctuations in psychosis: evidence from bipolar-schizophrenia network on intermediate phenotypes (B-SNIP) consortium. *Schizophr Bull* (2014) **41**(6):1336–48. doi:10.1093/schbul/sbv064
96. Ren W, Lui S, Deng W, Li F, Li M, Huang X, et al. Anatomical and functional brain abnormalities in drug-naive first-episode schizophrenia. *Am J Psychiatry* (2013) **170**(11):1308–16. doi:10.1176/appi.ajp.2013.12091148

Conflict of Interest Statement: The authors declare that the research was conducted in the absence of any commercial or financial relationships that could be construed as a potential conflict of interest.